ELSEVIER

Journal of Magnetism and Magnetic Materials 240 (2002) 420–422

Journal of magnetism and magnetic materials

www.elsevier.com/locate/jmmm

Growth and structural properties of Mn films on Si(1 1 1)–($\sqrt{3} \times \sqrt{3}$):Bi

G. Ctistis, U. Deffke, J.J. Paggel, P. Fumagalli

Freie Universität Berlin, Institut für Experimentalphysik, 14195 Berlin, Germany

Abstract

Mn films from the sub-monolayer to about 100 Å film thickness are grown on Si(1 1 1)–($\sqrt{3} \times \sqrt{3}$):Bi. Mn is observed to remove Bi from the surface reconstruction at room temperature, where Mn growth is polycrystalline. Annealing to 250°C leads to ordered films with a Si layer on top of a Mn film. Growth at elevated temperature results in a complicated sequence of two distinct Mn phases.

Keywords: Thin films—epitaxial structure

The increasing interest in spin-electronics or spintronics has led to the topic of spin injection into a semiconductor from a metal overlayer [1]. Experiments with metal layers generally show a very low asymmetry in the injected spin density. A much higher injected spin asymmetry is reported in the case of a semiconducting spin injector [2]. It is currently under discussion if this problem is related to the metallic nature of the contact or just to the bad quality of the interface layer. Interface roughness or unwanted chemical reactions at the interface might introduce a large probability for spin scattering (see for example, Refs. [3–5]). In search of a potential magnetic film material with an interface of good quality to a semiconductor material, the possibility of Mn growth on Si is investigated with unexpected results. Mn film growth on Si has so far been the target of only a few investigations and the main conclusion was the formation of a Mn silicide overlayer [6,7]. For "thicker" layers, i.e. more than just 1 or 2 ML, only a nonmetal to metal transition [8] and the growth of Mn silicide layers [9] has been reported.

The Mn films subject of this work are grown on the Bi-terminated ($\sqrt{3} \times \sqrt{3}$)-reconstruction of the surface. The native (7×7)-reconstruction is rather complex and possesses a large number of dangling bonds, rendering this surface rather reactive and leading to a number of interesting physical properties. The complicated atomic arrangement in the surface reconstruction leads to a large number of possible adsorption sites. This, together with the open atomic structure of the topmost atomic layer, lets the growth of smooth films and interfaces appear improbable. Mn growth on Si(1 1 1)–(7×7) is treated in a forthcoming publication [10]. Here we discuss film growth on the Bi-terminated, relatively closed surface reconstruction only.

Experimental methods involve Auger electron spectroscopy (AES), reflection high-energy electron diffraction (RHEED), and low-energy electron diffraction with spot-profile analysis (SPA-LEED). Mn films are grown from an electron-beam-heated Knudsen cell at a rate of about 0.13 Å/min and the film thickness is determined using a quartz microbalance. The vacuum system used is a standard oil-free molecular beam epitaxy (MBE) system equipped for the growth of metallic films. The system consists of a growth chamber, analysis chamber, and a fast-entry load lock. Pressure during film growth is below 1×10^{-9} mbar, while the pressure in the analysis chamber is in the 10^{-11} mbar range. Samples are mounted In-free on standard 2″ sample holders. Sample dimensions are limited to $12 \times 12\,mm^2$ for convenience. Sample heating is done with a radiative heater located at the back of the sample holder.

E-mail address: jens.paggel@physik.fu-berlin.de (J.J. Paggel).

0304-8853/02/$ - see front matter
PII: S0304-8853(01)00881-2

The Si(1 1 1)–(7×7) is prepared by thermal desorption of a clean chemically prepared oxide layer at a temperature of 1000°C in ultra-high vacuum with subsequent slow cooling of the sample to room temperature. The procedure routinely leads to the formation of a clean Si surface, as judged by AES and electron diffraction techniques. The surface is then exposed to a flux of Bi-atoms equivalent to a growth rate of ~0.5 Å/min at a temperature of ~500°C. The surface reconstruction changes from (7×7) to $(\sqrt{3}\times\sqrt{3})$:Bi by the incorporation of Bi-atoms. Roessler et al. identify three Bi-atoms per Si unit cell [11]. The surface is saturated with Bi and the coverage corresponds to one ML of Bi (according to our AES intensity calibration). The literature knows two Bi-induced reconstructions of $(\sqrt{3}\times\sqrt{3})$-symmetry (see for example Refs. [12–14] and references therein). As commented by Wan, the high-temperature preparation [12] leads to more reproducible results and is therefore better suited as a template for film growth.

The room-temperature deposition of 15 ML Mn on the Si(1 1 1)–$(\sqrt{3}\times\sqrt{3})$:R30°:Bi surface leads to amorphous films as visible in RHEED. Annealing the samples at 250°C for about 5 min leads to a well ordered and flat surface as observed using RHEED and LEED with domain sizes of the crystallites of ~50 Å (not shown here). Auger electron spectra taken from these films are shown in Fig. 1. The top trace shows a spectrum taken from a 15 Å thick film grown at room temperature. Mn and Bi dominate the spectrum, while no Si signal is visible. The Mn film covers the surface, and Bi is dissolved from the surface reconstruction at room temperature. Annealing the film to 250°C restores the Si signal, while part of the Bi-signal disappears (center trace). Increasing the film thickness to ~100 Å induces no change in the Auger spectra (Fig. 1 bottom), indicating that the chemical composition of the surface is either saturated or extremely inhomogeneous.

The kinetic energy of the Si-LVV peak from a film of even 100 Å thickness stays very close to the value it has in clean silicon (92 eV). Kawamoto et al. interpreted a component shifted by 10 eV as of silicide formation [8]. Straightforward, the observation of the Si-LVV component at the position of the Si bulk line leads to Si in a covalent bonding configuration. The origin of the unshifted peak could also be caused by large uncovered areas of the substrate, but the RHEED patterns show streaky structures, indicating a well ordered and flat surface. These facts lead to the conclusion that Si is floating on top of the Mn layer. A careful analysis of the Auger peak intensities points toward a 4 Å thick Si overlayer covering the Mn film.

Epitaxial growth of Mn on the Si(1 1 1)–$(\sqrt{3}\times\sqrt{3})$:R30°:Bi surface was achieved at a growth temperature of 250°C. The film exhibits sharp and well-ordered RHEED patterns through all coverage ranges. A collection of RHEED patterns taken at a beam energy of 30 keV in the $(1\,\bar{1}\,0)$-azimuth during growth is shown in Fig. 2. Fig. 2a shows the uncovered $(\sqrt{3}\times\sqrt{3})$:Bi surface. After the deposition of ~4 Å Mn, the RHEED pattern changes (not shown). Spots indicative of a 3-dimensional island growth appear. Upon further deposition, these spots become more intense, sharper, and a second line of spots becomes visible in the image (Fig. 2b). Analyzing these structures as bulk diffraction patterns leads to a lattice constant of ~12 Å in plane

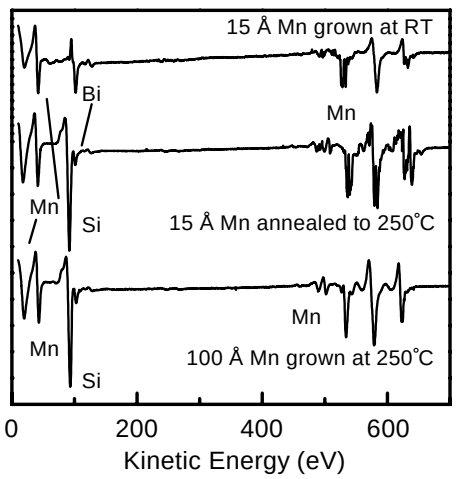

Fig. 1. A set of Auger spectra indicating the diffusion of the Bi and Si through the Mn layer: (a) 15 ML Mn on Si(1 1 1)–$(\sqrt{3}\times\sqrt{3})$:R30°:Bi grown at RT; (b) same sample as in (a) after annealing at 250°C; (c) a 100 Å thick Mn film grown at 250°C.

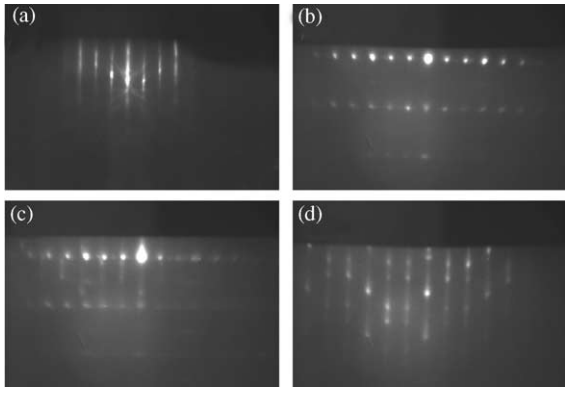

Fig. 2. RHEED patterns for the Si(1 1 1)–$(\sqrt{3}\times\sqrt{3})$:Bi reconstruction and Mn films grown on this reconstruction at a temperature of 250°C: (a) uncovered Si(1 1 1)–$(\sqrt{3}\times\sqrt{3})$:Bi surface in the $(1\,\bar{1}\,0)$ azimuth; (b) after about 10 Å of Mn are deposited on the surface, the truly 3-dimensional diffraction pattern develops; (c) at a Mn coverage of about 12 Å in addition to the spots, streaks appear; (d) after deposition of 14 Å Mn, the diffraction pattern shows all characteristics of a flat surface.

and ~4.5 Å out of plane. At a thickness between 11 Å and 13 Å, new spots appear at slightly different positions (Fig. 2c). With increasing film thickness, these spots gain in intensity and emerge into streaks dominating the image, which at a thickness of about 14 Å develop spots (Fig. 2d). These spots move along the streaks when the incident beam direction is varied, an indication of well-ordered 2-dimensional film growth. The lattice constant obtained from this pattern is ~11.5 Å, which is very close to the original periodicity of the Si substrate.

The evolution of the lattice constant mentioned above is shown in Fig. 3. The figure (right part) shows the RHEED intensity along a line along $k_{||}$ during film growth starting with the uncovered $(\sqrt{3}\times\sqrt{3})$-Bi surface up to a Mn thickness of about 15 Å. Fig. 3a shows selected slices at the indicated thickness. In the beginning, the streaks indicating the $(\sqrt{3}\times\sqrt{3})$-Bi structure disappear rapidly and at a thickness of ~4 Å, the new structure appears. Its lattice constant is about 5% larger than that of the $(\sqrt{3}\times\sqrt{3})$-reconstruction. This distance remains stable to a thickness of about 12 Å when the new pattern becomes visible (Fig. 2c). The streaks corresponding to this new structure have a larger distance again and match the positions of the substrate reflections. The film starts non-pseudomorphic in its own lattice parameter and seems to turn pseudomorphic after a critical thickness. It also starts with island growth mode and becomes more flat and well ordered with increasing thickness. The analysis of spot-profiles in LEED shows an increasing domain size from 40–50 Å for 15 Å thick films to more than 170 Å for the 100 Å thick Mn layer (not shown here).

Assuming a homogenous structure and chemical composition throughout the film, an enormous amount of elastic energy should build up if the film really turns pseudomorphic at about 14 Å-equivalent deposited Mn film thickness. This is not only unlikely, it contradicts the bulk of data from virtually all other growth studies. A more likely interpretation is that we in fact observe the fingerprints of a structural and also compositional phase transition or transformation as function of film thickness. All structures observed have three-fold symmetry. The observed lattice constant in the first phase of Mn growth corresponds to the lattice constant reported for the hexagonal compound Mn_5Si_3. This compound has a lattice constant of 6.910 Å in the (0 0 0 1) plane and 4.814 Å in the *c*-direction [15] and thus matches the Si superstructure within 4%. This so-called Nowotny-phase of the Mn_5Si_3 compound matches also the structural data obtained by other groups for the first phase of the Mn growth on Si(1 1 1) [7,9]. One, however, has to keep in mind that the topmost layer of the film presumably contains "pure" Si, which in turn leads to a reconstruction of the outermost surface layer, camouflaging the real periodicity in the film structure. The transition after 14 Å Mn growth then is probably due to the growth of "FCC-like" Mn [16] on Mn_5Si_3. The [1 1 1]-plane of FCC-Mn can form a coincidence lattice with the Mn_5Si_3 surface, i.e. a $\sqrt{27}\times\sqrt{27}$ superstructure of FCC-Mn matches the 2×2 unit cell of the Mn_5Si_3 compound. The resulting lattice parameters of 4.67 and 11.5 Å that are found in these structures are already known from the RHEED experiments.

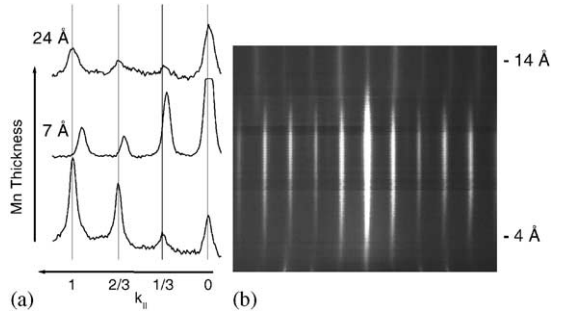

Fig. 3. RHEED intensity along the $(1\,\bar{1}\,0)$-azimuth as a function of Mn film thickness at a sample temperature of 250°C: (a) selected line scans, (b) grey scale representation of the scattered intensity.

This work is supported by the Deutsche Forschungsgemeinschaft through SFB 290.

References

[1] S. Datta, B. Das, Appl. Phys. Lett. 56 (1990) 665.
[2] B.T. Jonker, Y.D. Park, B.R. Bennett, H.D. Cheong, G. Kioseoglou, A. Petrou, Phys. Rev. B 62 (2000) 8180.
[3] G. Schmidt, D. Ferrand, L.W. Molenkamp, A.T. Filip, B.J. Wees, Phys. Rev. B 62 (2000) R4790.
[4] G. Kirczenow, Phys. Rev. B 63 (2001) 054422.
[5] E.I. Rashba, Phys. Rev. B 62 (2000) R16267.
[6] S.M. Shivaprasad, C. Anandan, S.G. Azatyan, Y.L. Gavriljuk, V.G. Lifshitz, Surf. Sci. 382 (1997) 258.
[7] M.M.R. Evans, J.C. Glueckstein, J. Nogami, Phys. Rev. B 53 (1996) 4000.
[8] S. Kawamoto, M. Kusaka, M. Hirai, M. Iwami, Surf. Sci. 242 (1991) 331.
[9] T. Nagao, S. Ohuchi, Y. Matsuoka, S. Hasegawa, Surf. Sci. 419 (1999) 134.
[10] G. Ctistis, U. Deffke, J.J. Paggel, P. Fumagalli, 2001, to be published.
[11] J.M. Roessler, T. Miller, T.-C. Chiang, Surf. Sci. 417 (1998) L1143.
[12] K.J. Wan, T. Guo, W.K. Ford, J.C. Hermanson, Phys. Rev. B 44 (1991) 3471.
[13] R. Shioda, A. Kawazu, A.A. Baski, C.F. Quate, J. Nogami, Phys. Rev. B 48 (1993) 4895.
[14] C. Cheng, K. Kunc, Phys. Rev. B 56 (1997) 10283.
[15] G.V. Samsonov, J.M. Vinitskii, Handbook of Refractory Compounds, Plenum Press, New York, 1980.
[16] D. Tian, S.C. Wu, F. Jona, Solid State Commun. 70 (1989) 199.